PM-IRRAS Spectroscopy for the Characterization of Polymer Nanofilms: Chains Conformation, Anisotropy and Crystallinity

T. Elzein, S. Bistac, M. Brogly, J. Schultz*

Institut de Chimie des Surfaces et Interfaces ICSI-CNRS, 15 rue Jean Starcky, 68057 Mulhouse, France
Fax: +33 3 89 60 87 99
E-mail: tamara_elzein@yahoo.fr

Summary: This paper is focused on the use of the Polarization-Modulation Infrared Reflection-Absorption Spectroscopy (PM-IRRAS) for studying thin polymer films at interfaces. When forming a polymer film on a metallic substrate, for instance by spin-coating, the characterization of the polymeric layer becomes very difficult given the small amount of matter deposited and also because of the contact with the metal. Among the techniques well adapted to surface and interface analyses, the PM-IRRAS spectroscopy represents an excellent tool to probe ultra-thin films.
Different systems have been selected in this study such as polyamides (PA) and ethylene-co-vinyl acetate (EVA) nanofilms spin-coated onto chemically controlled surfaces (i.e. thiol self-assembled monloayers grafted onto gold coated glass slides). PM-IRRAS spectroscopy allowed us to characterize the polymer anisotropy (chains orientation and conformation), to suggest a model for chain organization at the polymer/substrate interface, and to calculate the orientation angles. Moreover, we were able to determine, by using PM-IRRAS, the degree of crystallinity of PA and EVA films of nanometric dimensions without any calibration procedure needed by other techniques.

Keywords: conformation; crystalline; infrared spectroscopy; polymer; thin films

Introduction

Probing complex systems in terms of composition, conformation, and orientation exhibits an adapted technique such as infrared reflection- absorption spectroscopy (IRRAS) that allows a characterization going from organic surfaces to organic/inorganic interfaces [1]. The real potential of infrared reflection-absorption spectroscopy offers many advantages when analyzing organic films on metallic surfaces:

- The absence of specified experimental conditions (such as vacuum) during experiments.
- The non destructive nature of the infrared probe.

 DOI: 10.1002/masy.200450117

- The high spectral resolution.
- The possibility to work under high pressure for divers applications such as catalysis.
- And finally, the development of modulation techniques (PM-IRRAS: polarization-modulation IRRAS) that allows further applications, especially in terms of quantitative analyses for conformational studies. Moreover, ultra-thin films analysis becomes possible with the PM-IRRAS technique.

In this work, we will discuss the utility of the PM-IRRAS technique for the characterization of semi-crystalline polymer thin films adsorbed inert and functionalized gold coated substrates (by thiol grafting). The organization in the polymer layer is mainly defined by the chain orientation and conformation, by the crystallization and by the interfacial interactions established with the substrate in contact. The access to these different parameters was based on the PM-IRRAS experimental results. Two systems are studied: Polyamides (PA) and ethylene-co-vinyl acetate (EVA).

Materials

Thin films of PA (40 nm thick) were spin coated from 5g/l solutions (in trichloroethanol) on the chosen substrates (gold and thiol grafted gold substrates with OH, COOH and NH_2 functionalities). Acceleration, velocity and spinning time are respectively, 10^3 rpm/s, 2500 rpm and 60s. EVA thin films (22 nm thick) were spin coated from 5g/l solutions (in toluene for EVA9 and EVA14 and in chloroform for EVA24 and EVA28).

PM-IRRAS Technique

Usually, classic IRRAS experiments consist in recording the p-polarized reflectivity Rp(d) of the film on a metallic substrate and then normalizing it with respect to that of the bare substrate Rp(0). From these two different experiments one can compute the so-called IRRAS spectrum Rp(d)/ Rp(0). For overcoming the limitations of such an absolute reflectivity Rp measurement, polarization-modulation IRRAS was introduced to study thin films. Thus in PM-IRRAS a differential reflectivity ($\Delta R/R$) is obtained in one step and with all the dynamical range of the detection[2-5].

Measurements were done with an IF66S Bruker spectrometer; spectra were recorded with a MCT detector, under experimental conditions of 1000 scans, resolution of 1 cm^{-1}, 85° as beam angle of incidence and with a 74 kHz modulation frequency. A ZnSe photoelastic modulator provided by HINDS™ is used.

Briefly, the basic principle of the PM-IRRAS method is to combine the FT-IRRAS experimental conditions with a fast modulation of the polarization state of the incident electric field (ideally between p and s linear states) and to extract, from the detected intensity (using electronic filtering and demodulation), the two signals (R_p-R_s) and (R_p+R_s) in order to finally compute the differential reflectivity spectrum $\Delta R/R$.

This technique is based on three principles:

Selection rules induced by the reflection on metallic surface of infrared beam under grazing angles.

The double modulation of the incident beam.

The mathematical treatment of the detected signal in order to obtain the differential reflectivity:

$$\frac{\Delta R}{R} = \frac{R_p - R_s}{R_p + R_s} \qquad Eq.1$$

The big advantage of this technique is that the two reflectivities R_p and R_s are simultaneously obtained (i.e. during the same experiment).

PM-IRRAS selection rules implies that the sign and the intensity of an IR band is a function of the orientation of a transition moment (or functional group) relative to the surface plane. **Selection rules are then: if the orientation of a transition moment is parallel to the surface plane then the PM-IRRAS signal is equal to zero. If the orientation is perpendicular to the surface plane then the signal is maximum. Moreover, the contribution of the isotropic non-oriented phase into the global signal is eliminated in PM-IRRAS and thus this technique offers quantitative approach of the orientation angles.**

PM-IRRAS technique allows no environmental perturbation on the spectra and high signal to noise ratio. A background spectrum is typically taken to eliminate any instrumental artifacts.

Results and Discussion

In this part, each system will be discussed separately: PA and EVA.

PA:

IV.1.1. PA chains orientation[6,7]: To reach the chain orientation, one needs to compare bulk spectra considered as isotropic with those of thin films where the signal is a function of the molecular orientation. So, by comparing bands intensities of bulk PAs with their thin films (figure 1), and PAs this films spectra to each others, and by knowing the exact direction of vibrators with respect to the main chain axis and plane we were able to access an adsorption model of PAs chains in which we identified a rotation of the diacid/diamine planes (scheme 1).

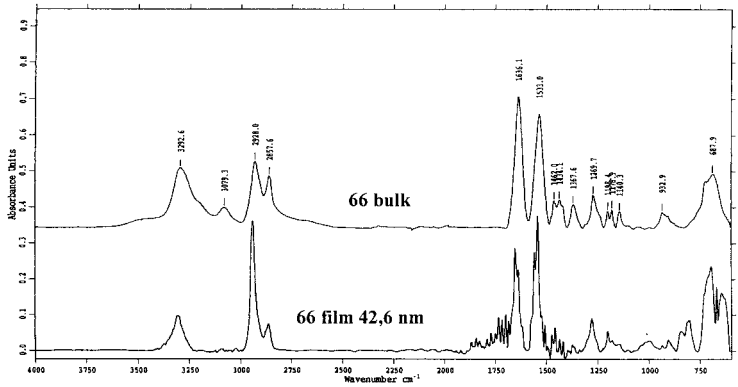

Figure 1: ATR spectra of bulk PA 66 compared with IRRAS spectra of 33nm thin film adsorbed on gold substrate.

On the basis of this qualitative model (scheme 1), it is possible to calculate the orientation angles ϕ and β representing respectively the diacid and diamine tilts with respect to the substrate normal. For that, we need to represent PA chains in geometrical referentials and to define, for each vibrator, the direction of its transition moment with respect to the normal in order to extract, for a given vibrator I, the geometrical functions F relating thin films bands intensities I_i with those of the bulk isotropic state A_i (Eq.2) :

$$\mathbf{I_i} \propto [\mathbf{F_i(\theta,\phi,\beta..)}]^2 . \mathbf{A_i} \qquad \text{(Eq.2)}$$

Referring to scheme 1 and applying equation 2 on infrared vibrators of PAs, we can establish the

following equations (3 & 4) that give ϕ and β in terms of bands intensities that are experimentally obtained from infrared spectra.

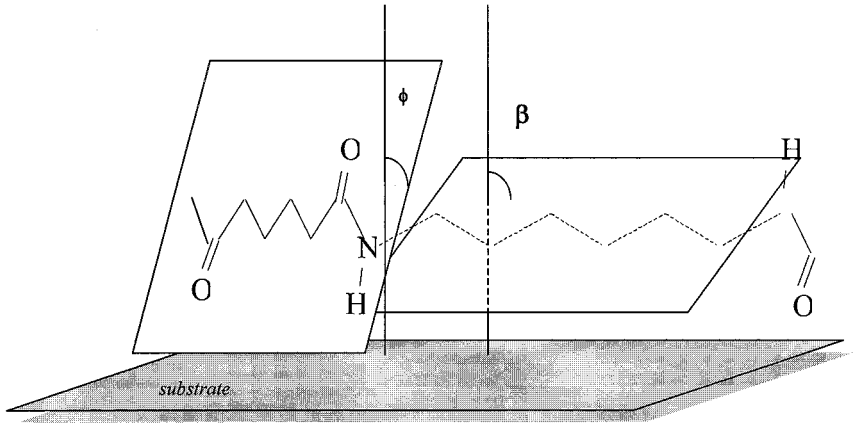

Scheme 1: Proposed model for chain conformation of adsorbed PA.

$$tg\phi = \sqrt{\frac{I(CH_2)as_{diacid}.A(NH)_b}{I(NH)_b.A(CH_2)as.K}} \qquad \text{(Eq. 3)}$$

$$\sin\beta = \frac{\sin\phi}{\sqrt{\frac{I(CH_2)as_{diacid}}{I(CH_2)as_{diamine}}\frac{K'}{K}}} \qquad \text{(Eq. 4)}$$

With these two relations, we calculated a value of 42° for ϕ, 62° for β and thus a rotation of about 20° of the diacid/diamine planes.

For a better comprehension of this new conformation, we needed to study PAs thin films crystallization.

PA thin films crystallinity[8,9]: taking into account that in the case of thin films, the degree of crystallinity (Xc) determination becomes very complicated, we looked for a calculation method based on infrared spectroscopy. For that, we should elaborate a calibration method with respect to

the bulk state, and thus we selected an infrared mode related to the crystalline phase such as bonded NH (because of the inter-chain hydrogen bonds in the PAs crystalline phase) and that we normalized by the symmetric CH2 mode. For chains involved in crystalline structures, the choice of symmetric mode is supported by the fact that in these PA chains, the CH2 symmetric stretching mode vibrates in the same direction than for the bonded NH stretching modes. In this case we avoid the orientation contribution in the thin films bands intensities.

This calibration allowed us to access to a relation that permits to calculate the degree of crystallinity Xc from bonded NH and symmetric CH_2 bands intensities (Eq. 5).

$$Xc = 0.919\ A(NH)_{bonded} / A(CH_2)s + 27.064 \qquad (Eq.5)$$

For thin films crystallinity measurements, we applied Eq.5 on the three PAs (adsorbed on gold and functionalized substrates), and the calculated values are compared in figure 2.

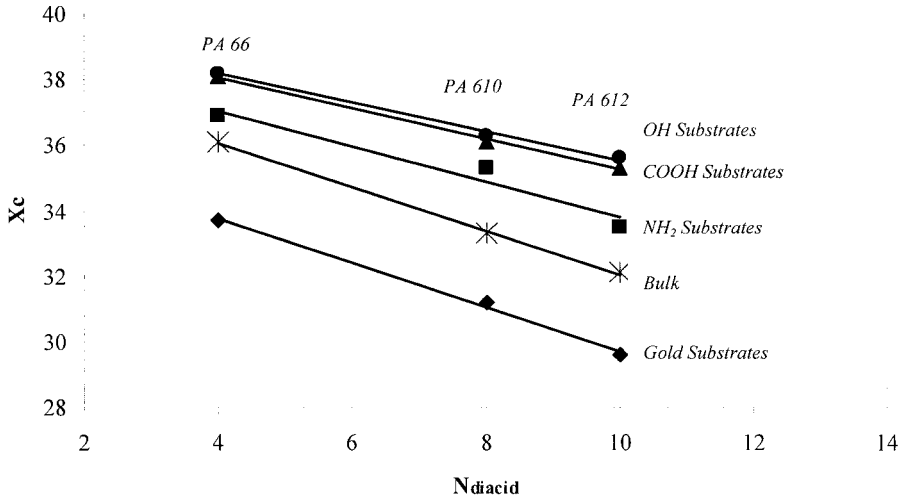

Figure 2: Comparison of Xc values of PAs: bulk and thin films

The comparison of these values indicates that Xc magnitude increases due to substrate functionalization, and highest values are obtained for OH and COOH grafts. When observing PAs

thin films morphologies (figure 3), we noticed dense structures of reduced spatial extension are observed for OH and COOH grafts, while big spherule and less dense structures are identified for NH_2. The high crystalline density observed in case of OH and COOH substrates confirms their highest Xc values. Apparently a high interfacial nucleation density is evidenced for OH and COOH compared to NH_2 substrates where spherule growth is favored (low nucleation density).

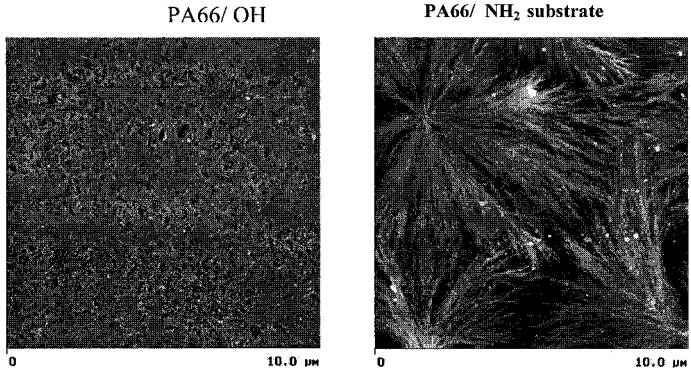

Figure 3: Morphological comparison of PA 66 adsorbed on OH and NH2 substrates

EVA:

EVA chains orientation[10]: the same procedure used for PA analysis is used in the case of EVA thin films. Our infrared analysis leads us to deduce that EVA chains lie parallel to the interface as shown in scheme 2.

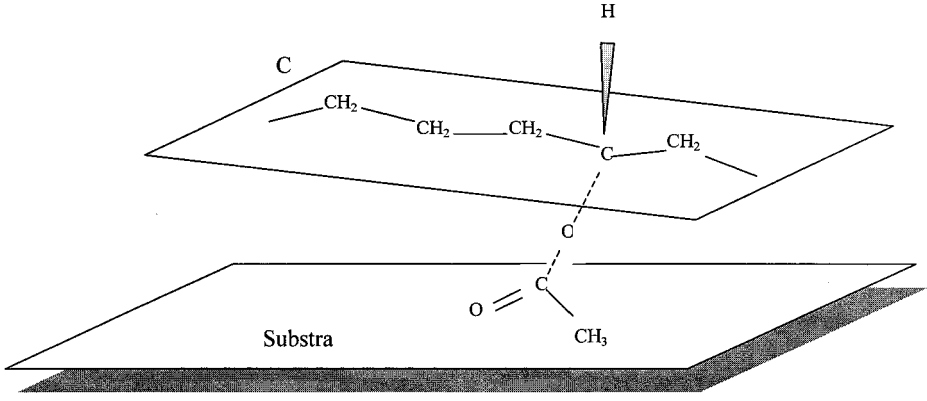

Scheme 2: Representation of EVA adsorbed chains

Calculated values of EVA orientation angles on gold and functionalized substrates revealed many observations:

- First, the main chain plane is oriented identically whatever the surface functionality is.
- Second, significant differences are observed for the acetate plane orientation especially in the case of EVA9 and EVA14. These differences were related to the interfacial interactions established between the EVA C=O groups and the surface grafts. Such interactions are well identified on IR spectra in the C=O absorption region: the C=O band is splitted in two components, free and acid-base one.

Moreover, these interfacial interactions could induce changes during EVA thin films crystallization.

EVA thin films crystallinity[11]: We choosed to calibrate the crystallinity with a crystalline band such as $s(CH_2)$ at 1467 cm^{-1} normalized by another mode used as internal reference. This latter should satisfy two conditions:

- Its transition moment should vibrate in the same direction of $s(CH_2)$, in order to avoid orientation contributions in thin films.
- It should belong to the crystalline phase so its intensity within the thin film is not affected by the disappearance of the amorphous phase signal (since that in the case of EVA thin films the PM-IRRAS response is limited to the crystalline region).

On the basis of these conditions, one internal reference could be chosen: the crystalline asymmetric CH_2 stretching mode $\nu(CH_2)as_{cr}$ that vibrates in the same direction than the $s(CH_2)_{cr}$ mode.

With this calibration, we established four equations for the four EVA (Eq.6-9).

EVA9 nanofilms : $$X_c = 0.32 \frac{Is(CH_2)_{cr}}{I(CH_2)as}$$ Eq. 6

EVA14 nanofilms : $$X_c = 0.28 \frac{Is(CH_2)_{cr}}{I(CH_2)as}$$ Eq. 7

EVA24 nanofilms : $$X_c = 0.18 \frac{Is(CH_2)_{cr}}{I(CH_2)as}$$ Eq. 8

EVA28 nanofilms : $$X_c = 0.05 \frac{Is(CH_2)_{cr}}{I(CH_2)as}$$ Eq. 9

Calculated values of EVA thin films crystallinity degrees are compared with the bulk ones in the next table (table 1).

Table 1. Xc values of EVA thin films. G, C and N are used to note the surface chemistry respectively for gold, COOH and NH_2 substrates.

Thin Film	Xc (%)	Xc bulk (%)
E9G, E9C, E9N	*11*	33.1
E14G, E14C, E14N	*9*	28.6
E24G, E24C, E24N	*6*	22.1
E28G, E28C, E28N	*2*	12.4

This crystallinity reduce of EVA thin films after adsorption could be justified by taking into account the presence of interfacial interactions: one way for EVA chains to satisfy a high density of interfacial intercation sites is to rearrange conformations to form loops and trains at the interface. Such conformations (loops and trains) are very unfavored for chains crystallization (nucleation and growth). The low crystallinity was also confirmed by AFM: when imaging the surface at various scales we deduced that no lamellar morphologies are developed, and that whatever is the substrate chemistry. As a consequence, these reduced structures and the absence of well organized entities in EVA nanofilms leads us to confirm the amorphization and the low crystallinity degrees calculated by PM-IRRAS.

Conclusion

In this work, we showed that PM-IRRAS spectroscopy is an excellent tool for ultra-thin polymer films analysis. It is a powerful technique for orientation and conformation studies and offers the possibility to access quantitative calculation of orientation angles. Moreover, we developed this technique for studying polymer thin films crystallization by elaborating calibration methods allowing for crystallinity measurements.

[1] M.K. Debe, *Appl. of Surf. Sci.* **1982**, *14*, 1.
[2] T. Buffeteau, B. Desbat, M. Pézolet, J.M. Turlet, *J. Chim. Phys.* **1993**, *90*, 1467.
[3] T. Buffeteau, B. Desbat , J. Devaure, A. Salimi, J.M. Turlet, *J. Chim. Phys.* **1993**, *90*, 1871
[4] T. Buffeteau, B. Desbat, M. Pézolet, J.M. Turlet, *Appl. Spectrosc.* **1991**, *45*, 380.
[5] T. Buffeteau, B. Desbat, E. Péré, J.M. Turlet, *Mikrochim. Acta* **1997**, *14*, 627.
[6] T. Elzein, M. Brogly, G. Castelein, J. Schultz, *J. of Polymer. Sci.* **2002**, *40*, 1464.
[7] T. Elzein, M. Brogly, J. Schultz, *Polymer* **2003**, *43*, 3649.
[8] T. Elzein, M. Brogly, J. Schultz, *Polymer* **2002**, *34*, 4811.
[9] T. Elzein, M. Brogly, J. Schultz, *J. Surf. Interf. Anal.* **2003**, *35*, 231.
[10] T. Elzein, M. Brogly, J. Schultz, *J. Surf. Interf. Anal.* **2003**, in press.
[11] T. Elzein, M. Brogly, J. Schultz, *Surf. Interf. Anal.* 2003, submitted.